Overview of measurements performed by the Raman Lidar BASIL in the frame of the Convective and Orographically-induced Precipitation Study

Paolo Di Girolamo[1], Donato Summa[1], Rohini Bhawar[1], Tatiana Di Iorio[2], Marco Cacciani[2], Igor Veselovskii[3], Alexey Kolgotin[3] Evelyne Richard[4], Geraint Vaughan[5], Emily Norton[5], Gerhard Peters[6]

[1] *DIFA, Università degli Studi della Basilicata, Potenza, Italy,*

[2] *Dipartimento di Fisica, Università degli Studi di Roma "La Sapienza", Roma, Italy*

[3] *Physics Instrumentation Center, Troitsk, Moscow Region, Russia*

[4] *Laboratoire d'Aerologie, Toulouse, France*

[5] *School of Earth, Atmospheric & Environmental Sciences*
Simon Building, University of Manchester, Manchester M13 9PL, UK

[6] *Meteorologisches Institut, Universität Hamburg,*
Bundesstraße 55, D 20146 Hamburg, Germany

7th COPS Workshop, 27-29 October 2008, Strasbourg, France

BASIL Raman Lidar

Measured parameters:

- particle backscattering coeff. @ 355, 532 and 1064 nm 3β
- particle extinction coeff. @ 355 and 532 nm 2α
- depolarization ratio @ 355 & 532 nm,
- atmospheric temperature
- water vapour mixing ratio
- relative humidity from simultaneous measurements of temperature and water vapor mixing ratio

particle size and microphysical parameters

COPS Web Page
http://www.cops2007.de/
Operational Products

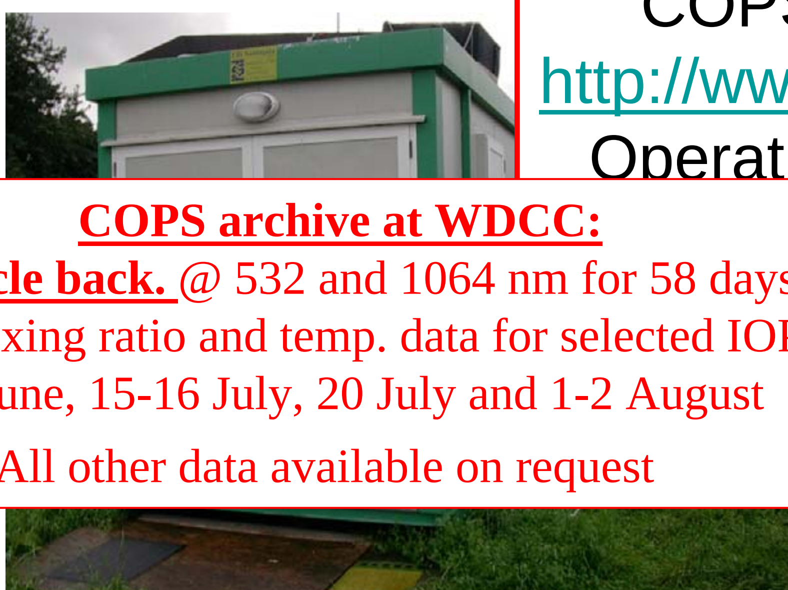

COPS archive at WDCC:

Particle back. @ 532 and 1064 nm for 58 days
2O mixing ratio and temp. data for selected IOPs:
20 June, 15-16 July, 20 July and 1-2 August

All other data available on request

Raman lidar measurements
(25 May – 30 August 2007)

More than 500 hours of measurements distributed over 58 days

Observation of a Saharan dust outbreak on 1-2 August 2007
Determination of size and microphysical particle parameters

Particle Backscatter Ratio at 1064 nm, 1-2 August 2007

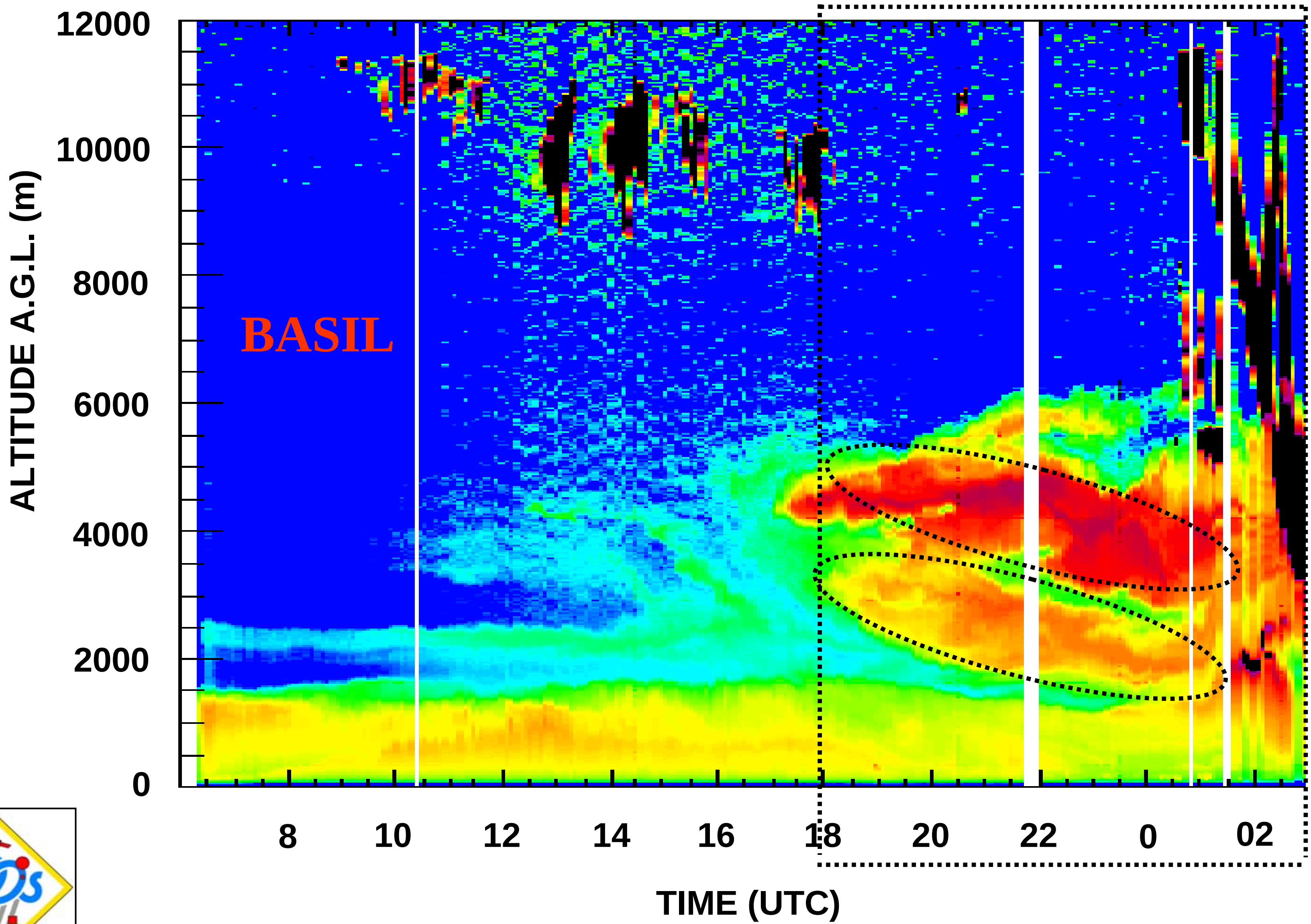

Water Vapour Mixing Ratio

1-2 August 2007

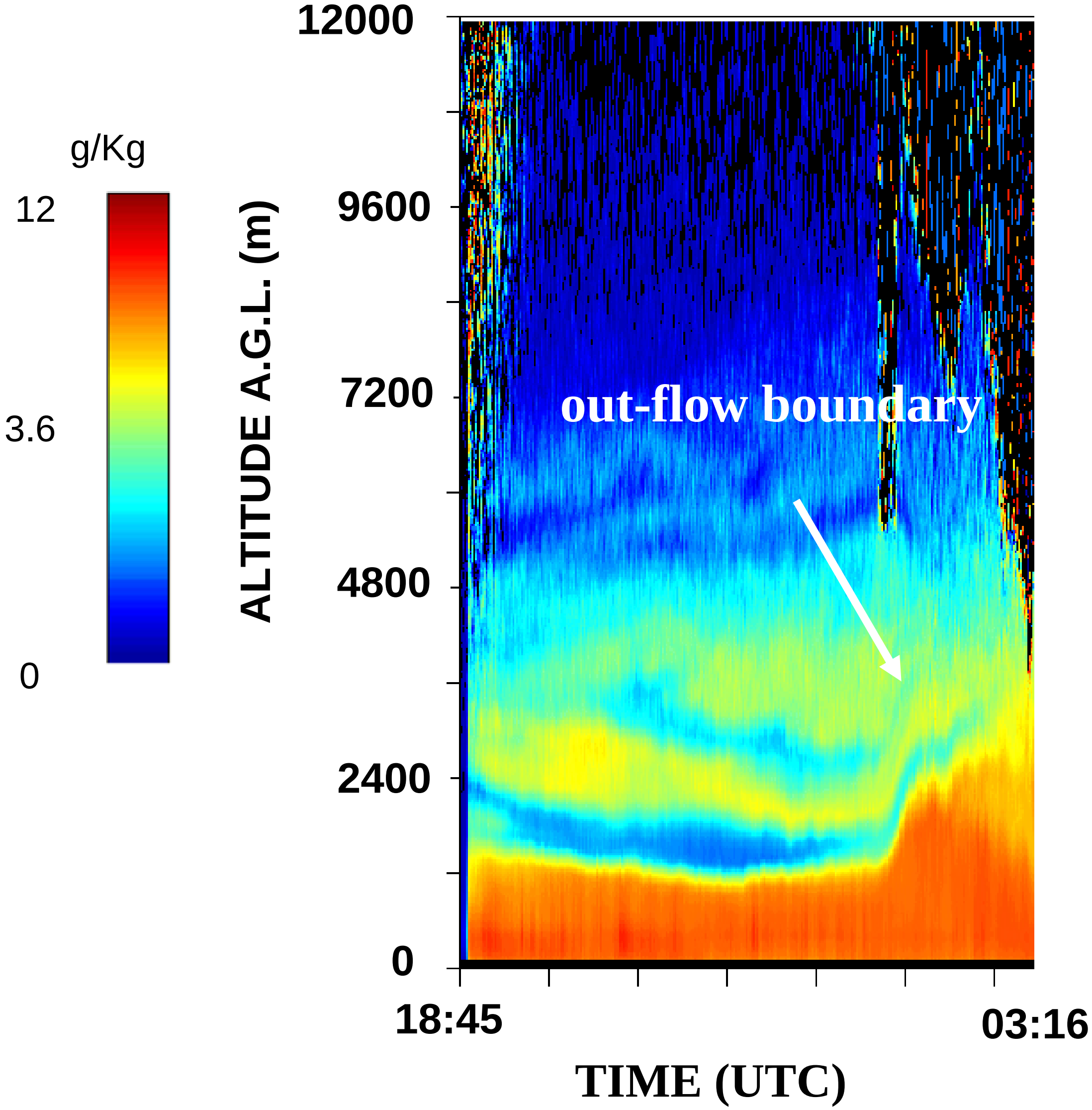

Inversion algorithm

$3\beta + 2\alpha$

Particle size distribution parameters:

Mean radius $\mathbf{r_{mean}}$

Effective radius $\mathbf{r_{eff}}$

Number concentration **N**

Surface concentration **S**

Volume concentration **V**

Complex refractive index $\mathbf{m_r}$ and $\mathbf{m_i}$

Parameters of a bimodal size distribution

The retrieval scheme employs Tikhonov's inversion with regularization

Algorithm developed at the Physics Instrumentation Center

Veselovskii et al., Appl. Opt. **41,** 3685–3699, 2002.

In the solution of the inverse problem, particle size distribution *f(r)* is approximated by the superposition of base functions $B_j(r)$ as:

$$f(r) = \sum_{j=1}^{q} c_j(z) B_j(r)$$

where $c_j(z)$ are the weight coefficients.

Base functions have a triangular shape on a logarithmic-equidistant grid

Inversion with regularization

r_{min}=0.05 μm, r_{max}=15 μm

$1.3 < m_r < 1.6$

$0 < m_i < 0.04$

f(r) →

- Mean radius **r_{mean}**
- Effective radius **r_{eff}**
- Number concentration **N**
- Surface concentration **S**
- Volume concentration **V**

$$r_{eff} = \frac{\int_{r_{min}}^{r_{max}} r^3 f(r)dr}{\int_{r_{min}}^{r_{max}} r^2 f(r)dr} \qquad r_{mean} = \frac{\int_{r_{min}}^{r_{max}} rf(r)dr}{\int_{r_{min}}^{r_{max}} f(r)dr}$$

numerically integrating *f(r)* over the size interval [r_{min}, r_{max}]

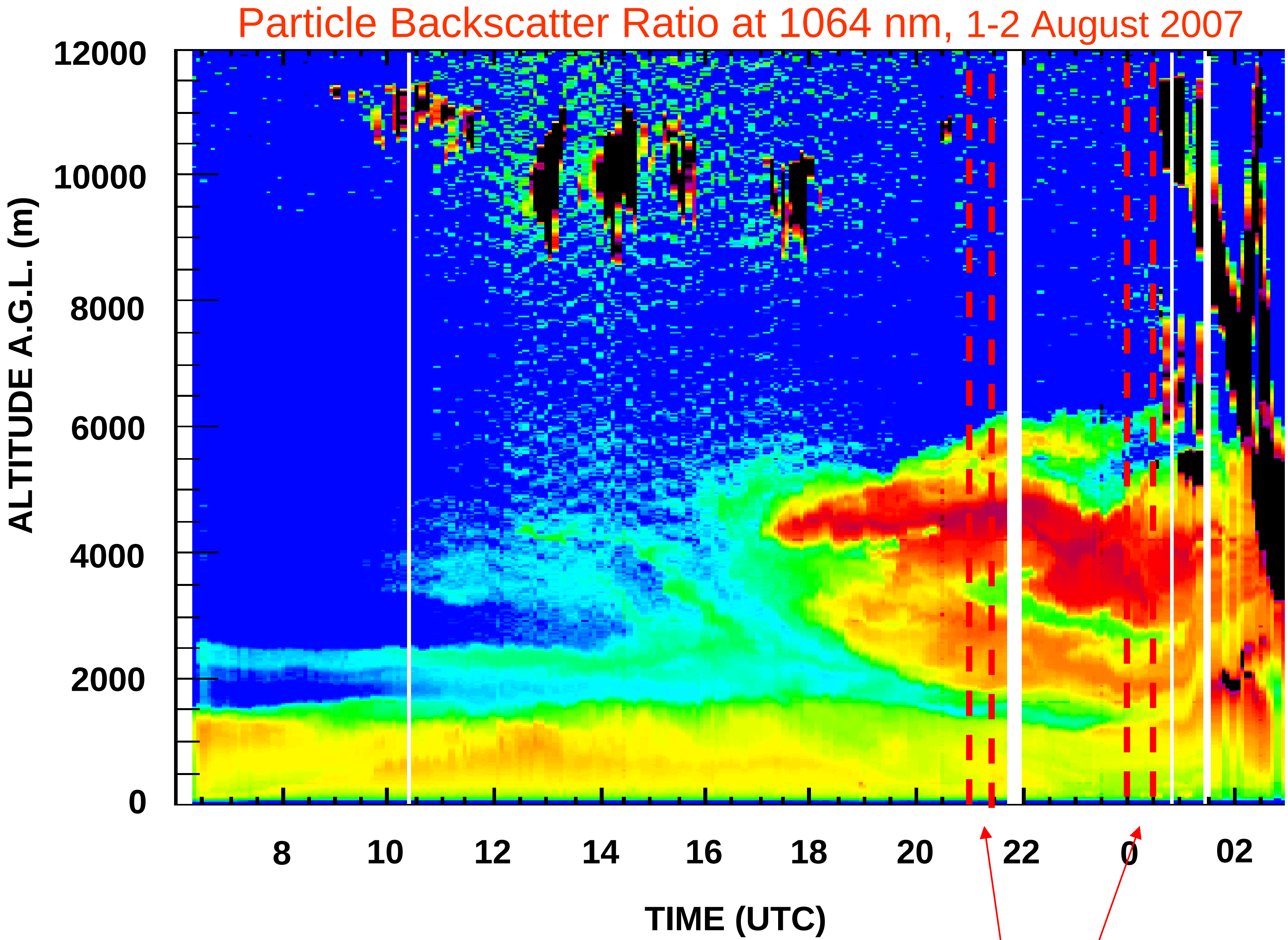

Focus: two specific times when aerosol loading was higher

21:00-21:30 UTC on 1 August 2007

00:00-00:30 UTC on 2 August 2007

(red dashed lines in figure)

1 August 2007, 21:00-21:30 UTC **2 August 2007, 00:00-00:30 UTC**

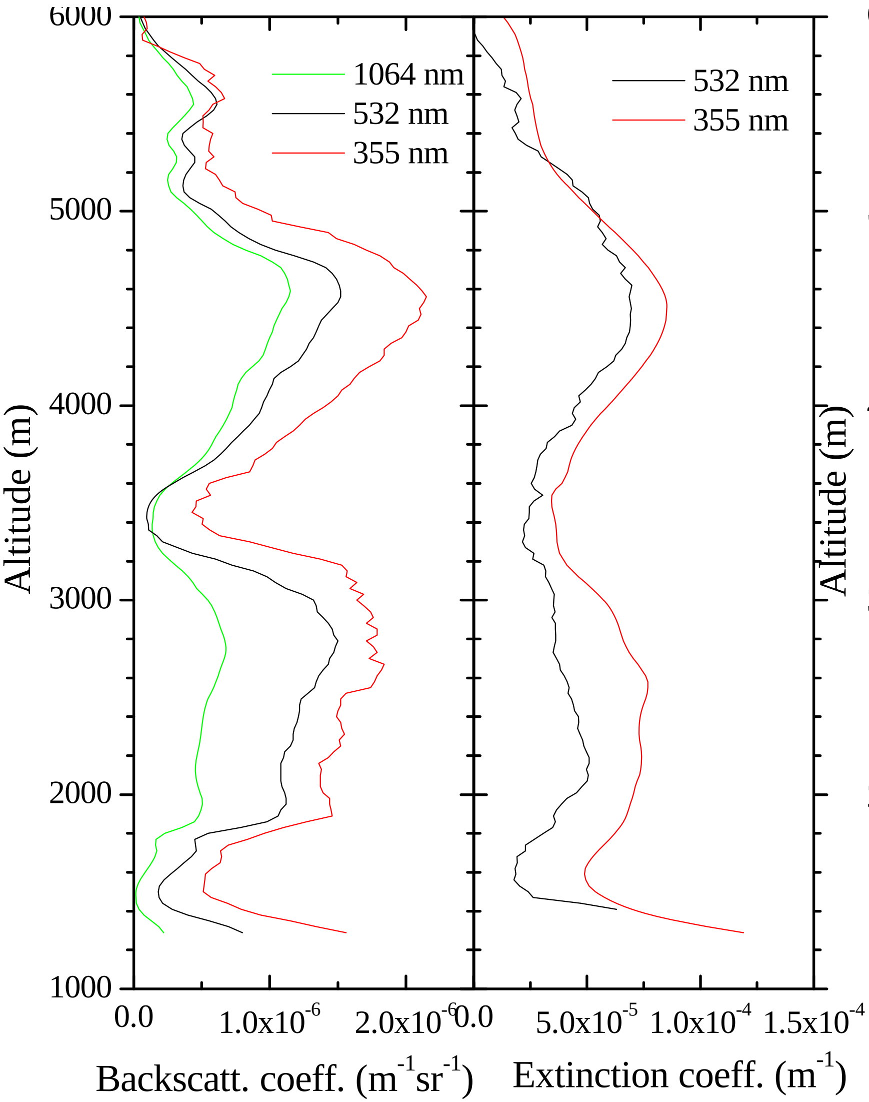

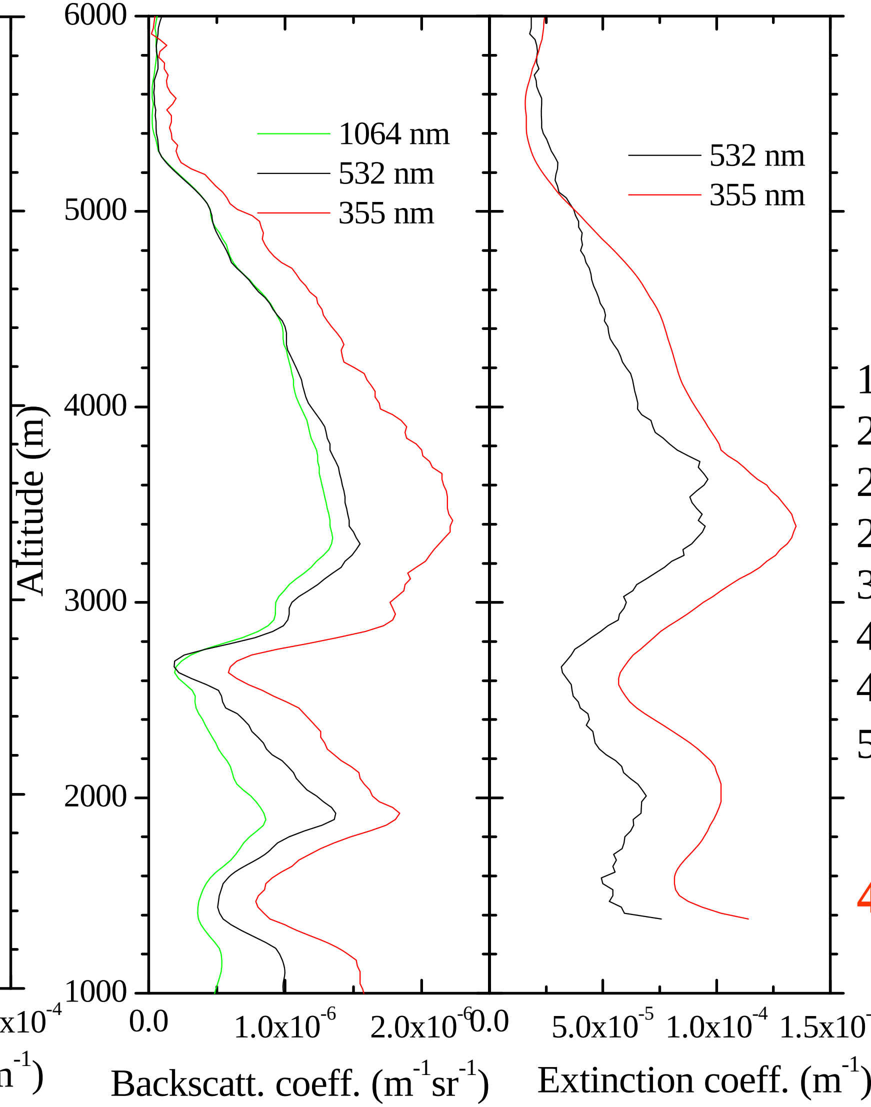

averaging layers

1710-2100 m
2100-2490 m
2490-2910 m
2910-3210 m
3690-4110 m
4110-4500 m
4500-4920 m
5310-5700 m

400 m thick

1 August 2007, 21:00-21:30 UTC

2 August 2007, 00:00-00:30 UTC

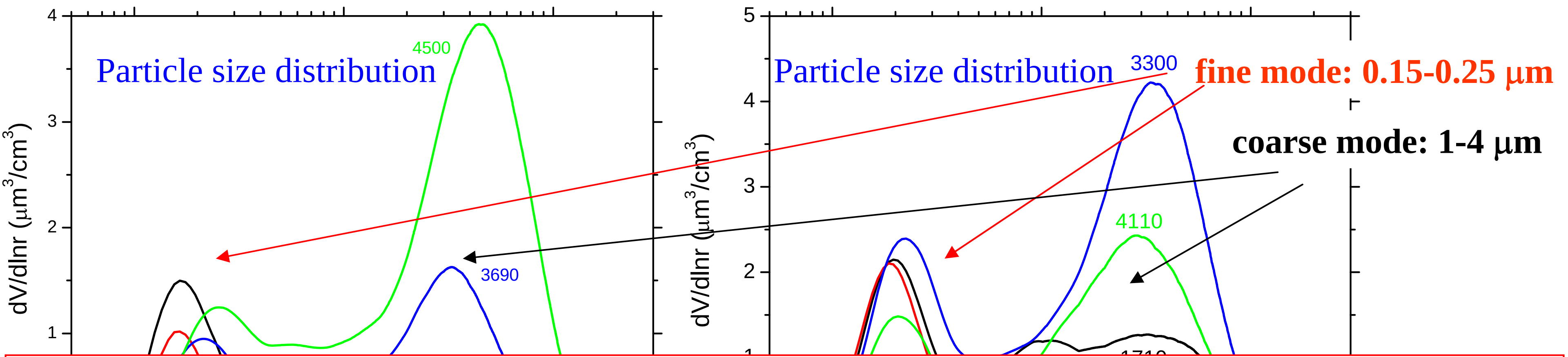

Dust particles ⟷ non-spherical ⟷ Retrieval of particles parameters challenging

Mie kernel functions for spherical particles may not be appropriate for dust particles

Presently, we are developing **phase functions of dust part.** considering **ensemble of spheroids**

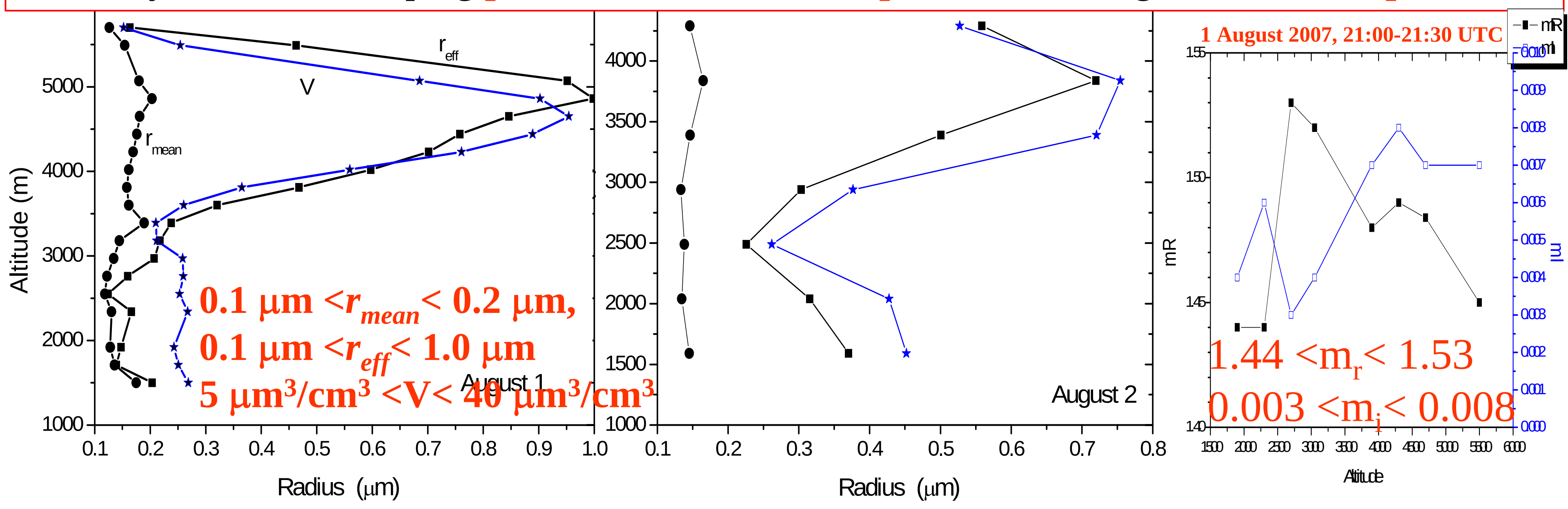

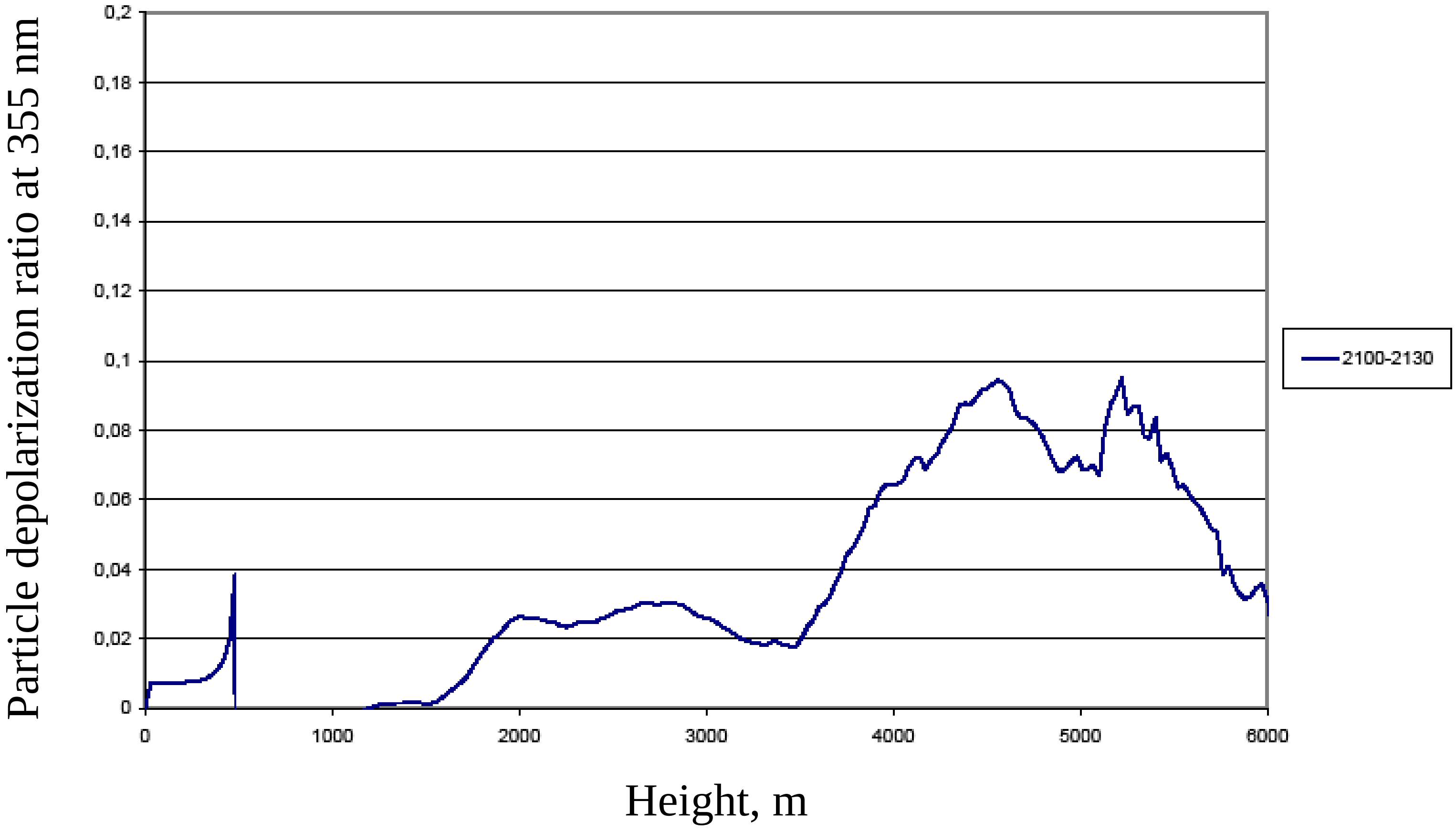

Low depolarization values in the lower layer

Backward trajectories ending at 00:00 UTC on 2 August 2007

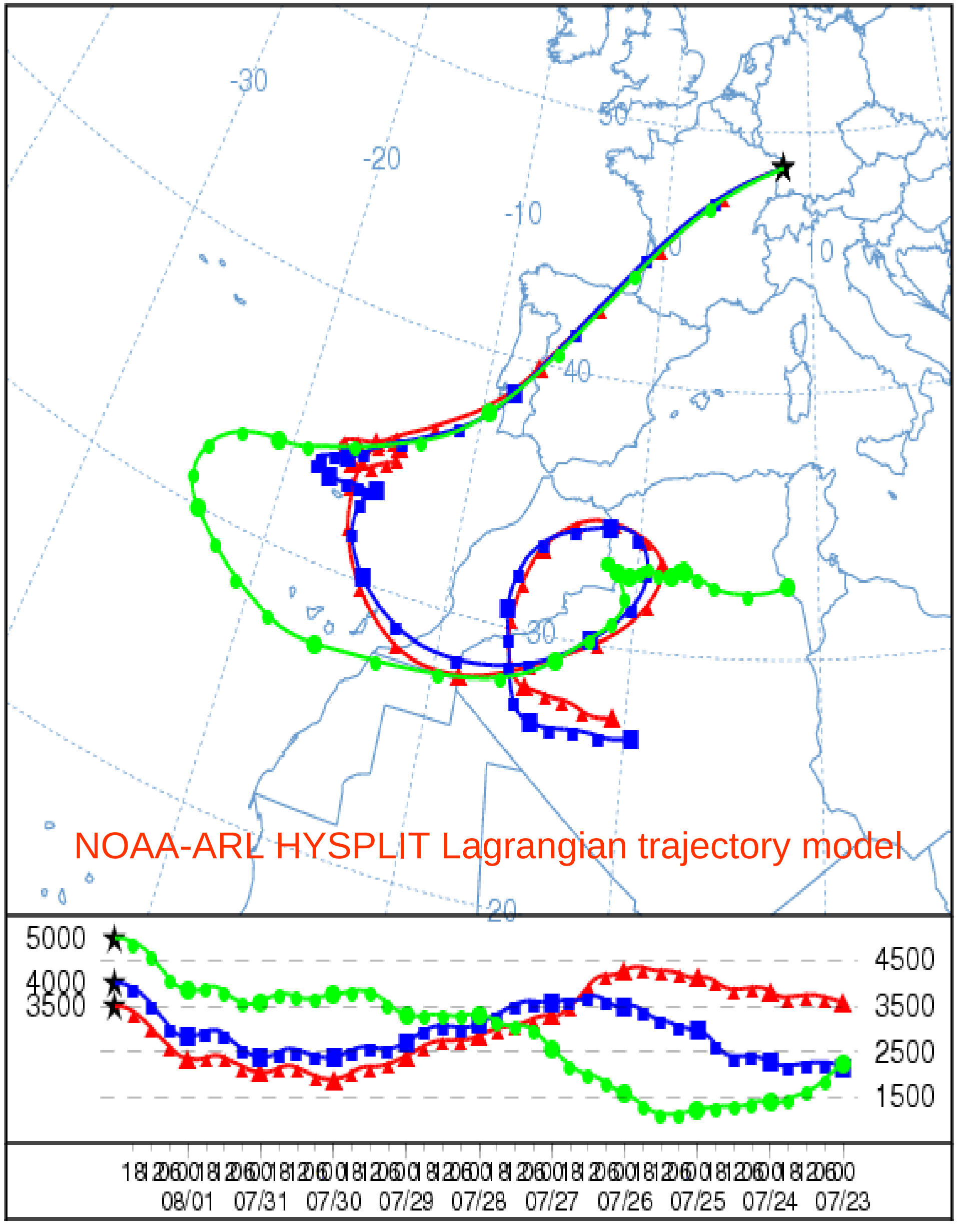

The air masses observed in Achern in the altitude region 3.5-5 km a.g.l. originated in the mixed layer over the Saharan desert

Particle backsc. coeff. at 355 nm vs RH

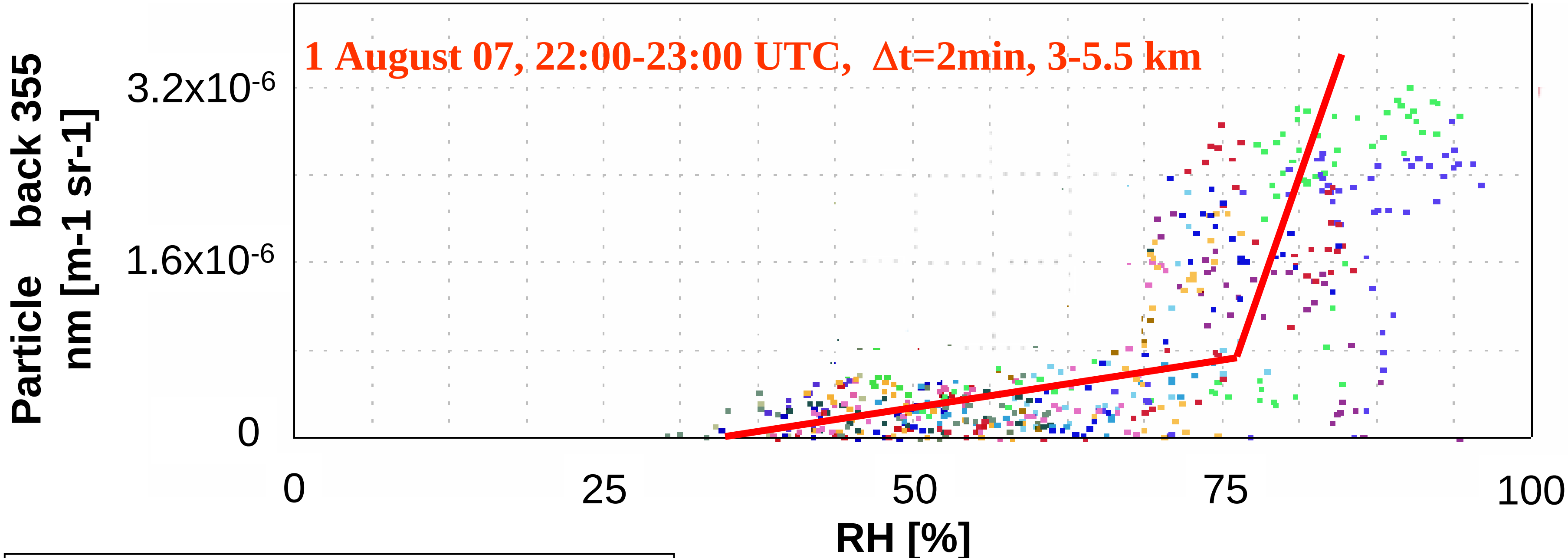

Substantial increase in particle backscattering when RH > 75 %

Swelling tendency of hygroscopic aerosol particles at large RH values

Trend compatible with partially soluble aerosol particles

Back-trajectories show that airmasses originated in the Saharan desert transited for several days over the Atlantic Ocean

Aged dust particles presumably mixed with maritime aerosol during the advection to the meaurement site and partially coated with hygroscopic material

Lidar and radar measurements in the melting layer: observations of dark and bright band phenomena

Changes in scattering properties of precipitating particles take place during the snowflake-to-raindrop transition, near the 0^0C isotherm.

- **Maximum** in **radar reflectivity** at microwave wavelengths (**Radar bright band**).
- **Minimum** in **particle backscatter** in the optical domain (**Lidar dark band**, *Sassen and Chen, 1995)*

Lidar dark band

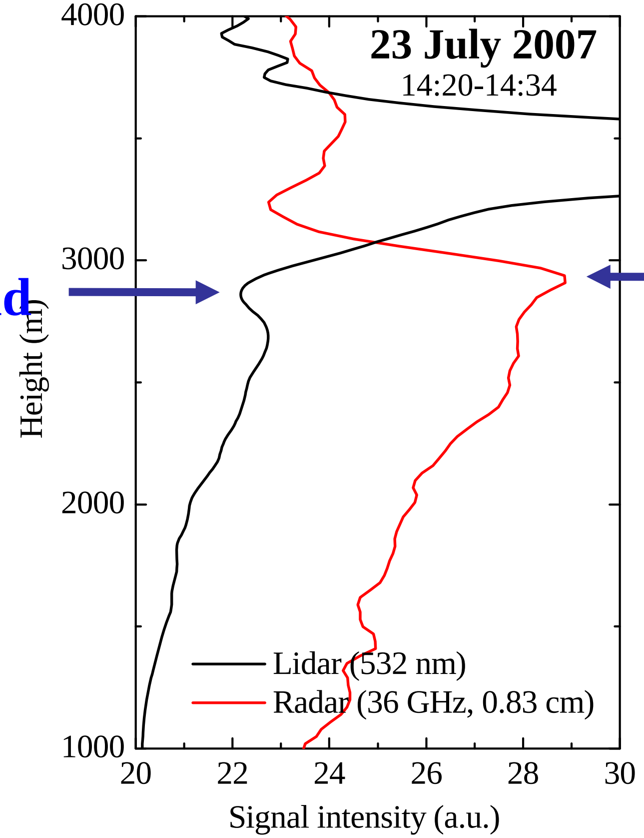

Radar bright band

Instruments considered

Lidar measurements supported by:

- Cloud radar MIRA 36 (36 GHz, 0.83 cm, Ka-band), Univ. of Hamburg
- Dual-polarization micro rain radar (24.1 GHz, 1.24 cm, K-band), Univ. of Hamburg
- Clear air wind profiler (1.29 GHz, 23.24 cm, UHF band), the Univ. of Manchester

Unique data set → None of the previous reported measurements could rely on:

- MW lidar backscatter, extinction and depolarization data,
- MW radar reflectivity, depolarization and Doppler velocity data

Additional ancillary information on the state of the atmosphere was provided by:

- Radiosondes, launched every three hours during each measurement session
- Sodar
- Microwave radiometer
- Disdrometer

This large "ensemble" of instruments makes the collected dataset unique for the study of precipitating hydrometeors in the melting layer.

23 July 2007

BASIL Raman Lidar

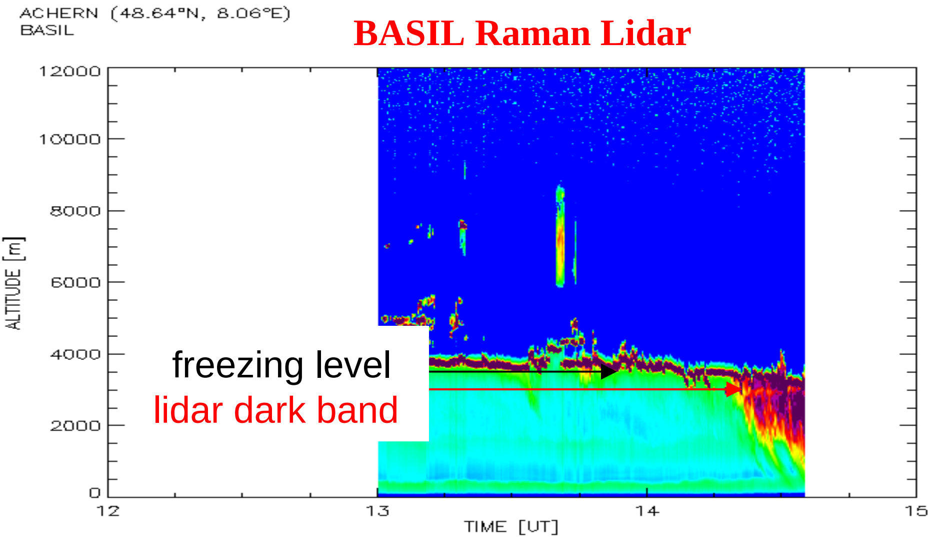

University of Manchester Radio Wind Profiler, 1290 MHz UHF Doppler radar

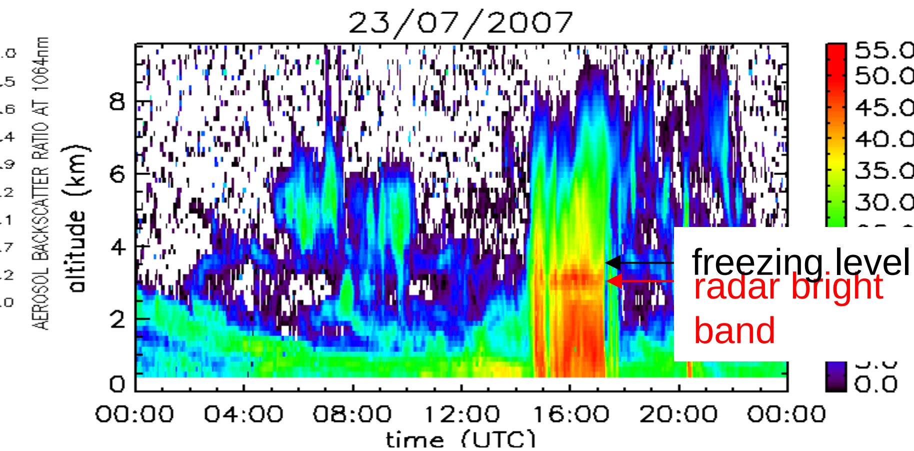

MIRA 36, Radar Reflectvity at 36 GHz

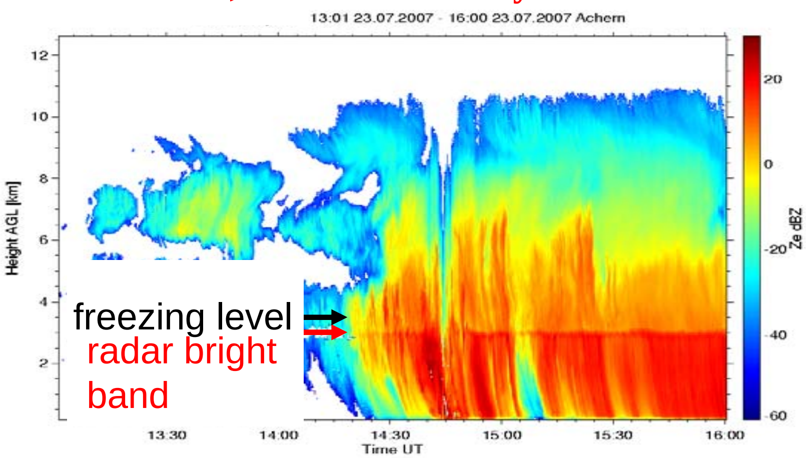

MIRA 36, Linear Depolarizatio Ratio

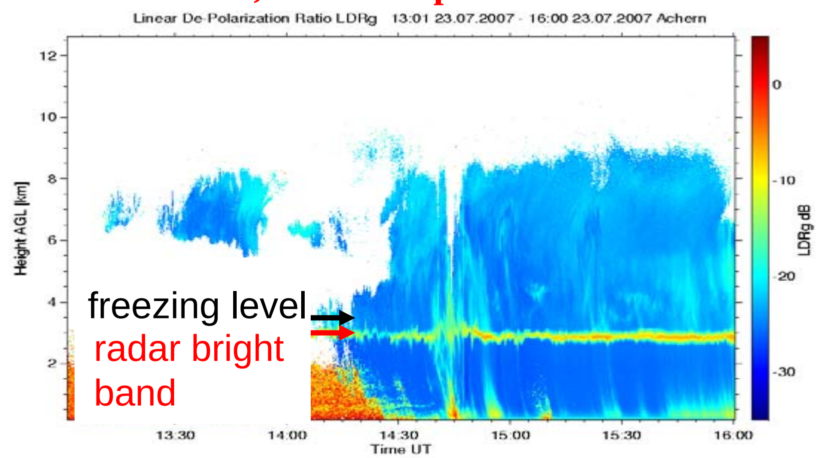

23 July 2007

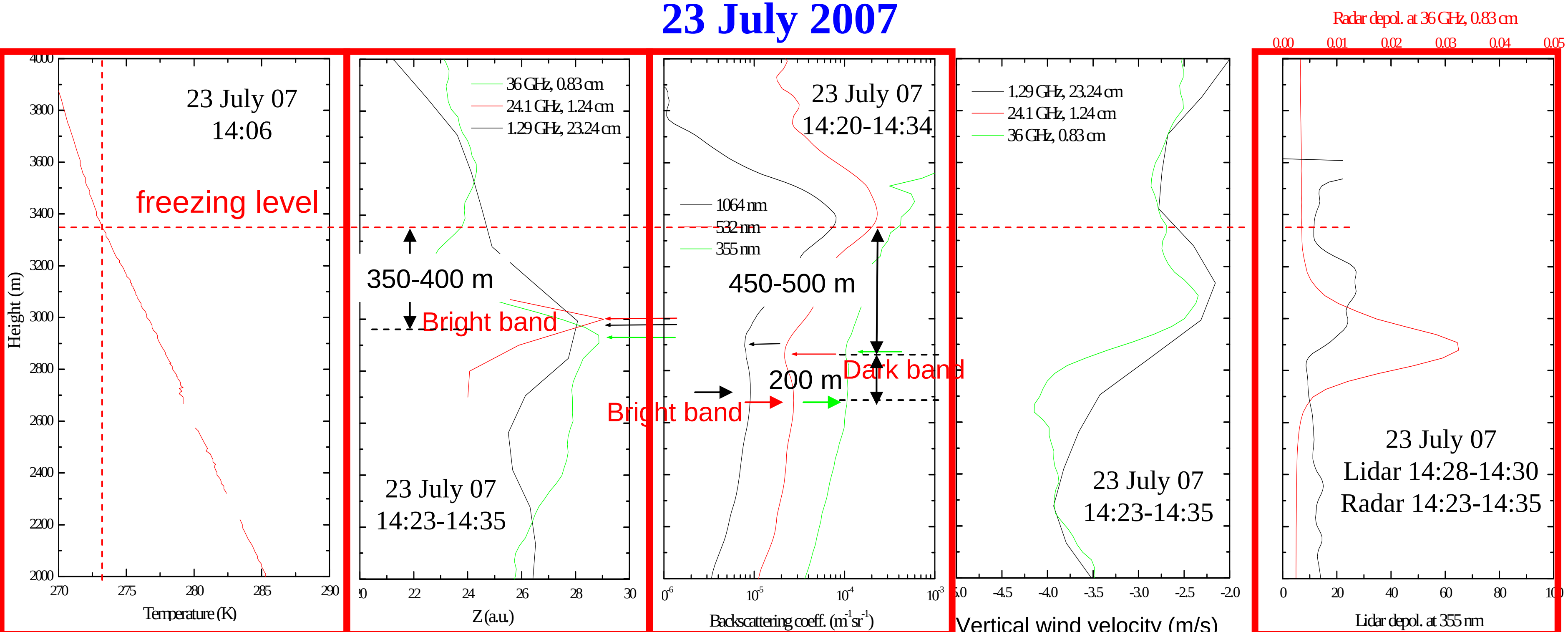

Temperature	Radar Z Height	Lidar Range below 0 ^{0}C	Vert. wind Temperature	depol
Freezing level	~ 3350 m a.g.l.	-		
Radar bright band	2950-3000 m a.g.l.	350-400 m	3.4 - 3.9 ^{0}C	276.5-277.0 K
Lidar dark band	2850-2900 m a.g.l.	450-500 m	4.4 - 4.9 ^{0}C	277.5-278.0 K
Lidar bright band	2700-2750 m a.g.l.	600-650 m		
Lidar depol	25-30 % @ 3200 m, ~ 10 % @ 2850 m a.g.l.			
Radar depol	peak @ 2900 m a.g.l.			

Radar Doppler velocity (@) reaches its plateau @ 2600-2700 m

Unexpected low values of lidar depolarization at the height of the lidar dark and bright bands, which may imply that precipitating particles are almost spherical or have a more regular shapes.

Simulation approach:

We combine:
- a Mie scattering code
- melting layer model

Mie computations based on a concentric/eccentric sphere code

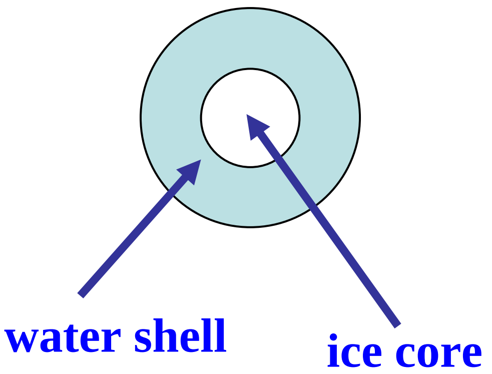

- **Mie code for large particles with off-centre inclusions**
- **Ice core at the top/bottom of the water shell.**

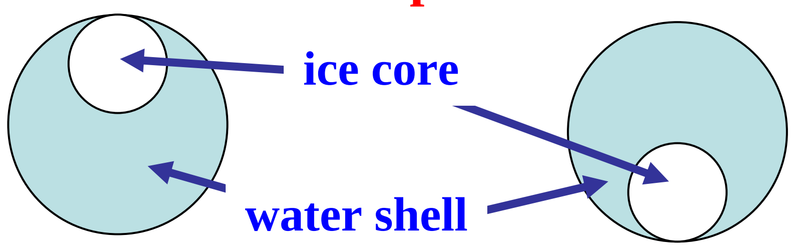

Backs. Coeff. at 0.35 µm versus core/shell radius ratio r_c/r_s

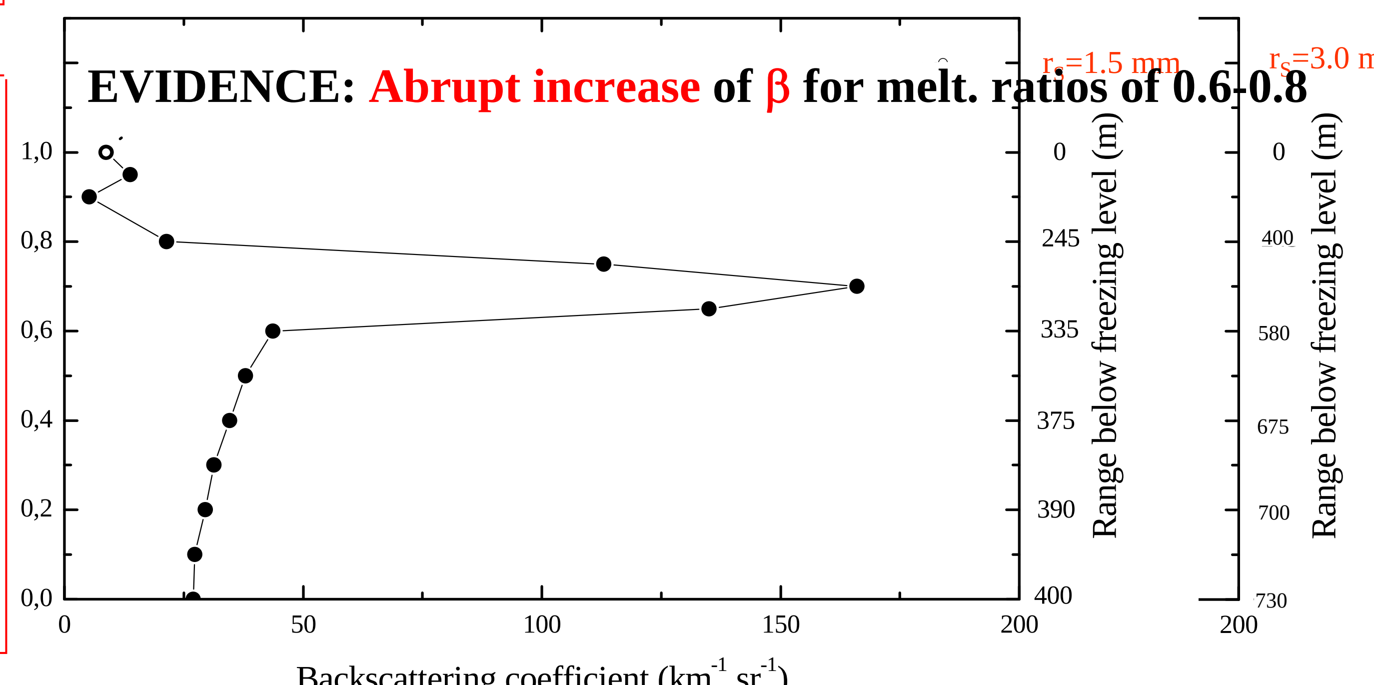

Melting hydrometeor model:

water shell + ice core

(Yokoyama and Tanaka, 1984; Olson et al., 2001)

Simplified and schematic conceptual representation

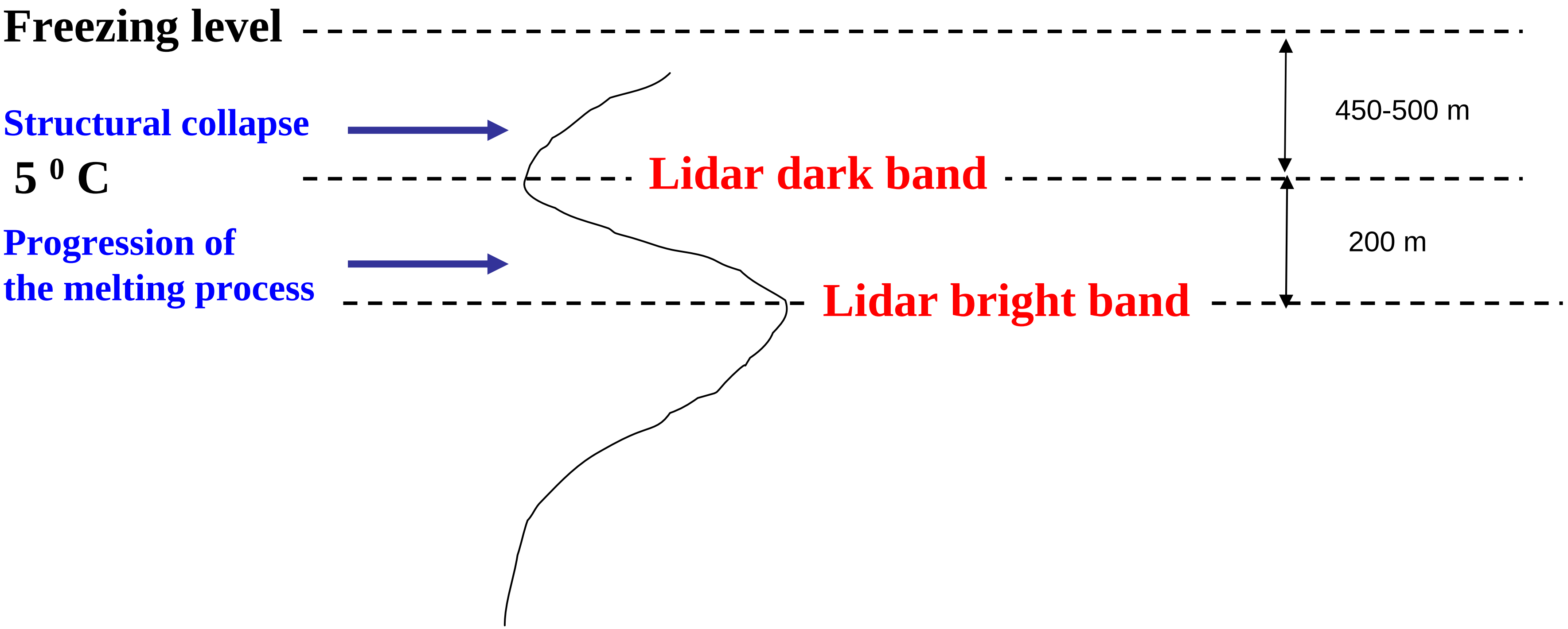

Lidar dark band → Structural collapse of partially melted snowflakes, leading to a decrease of lidar backscattering as a result of the reduced particles size and concentration (approx. 450-500 m below the freezing level)

Lidar bright band → Progression of the melting process, leading to a sudden increase of lidar backscattering when melting ratio is smaller than 0.8.

Comparison on water vapour and aerosol measurements from the Raman lidar BASIL with runs from Meso-NH model and other mesoscale models

Water Vapour Mixing Ratio, BASIL - Rhine Valley Supersite, 15 July 2007

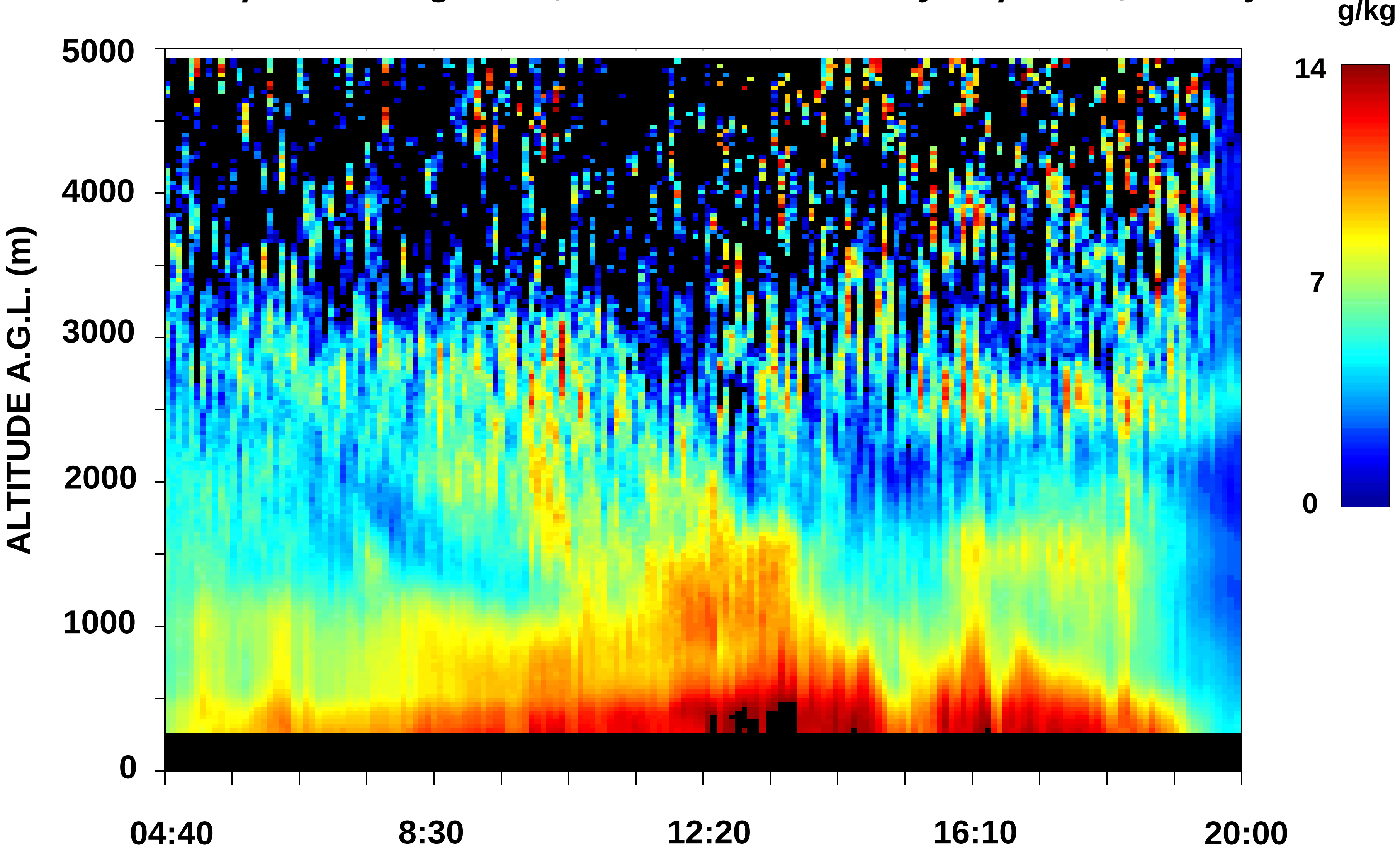

ΔT: 5min

Comparison on water vapour and aerosol measurements from the Raman lidar BASIL with runs from mesoscale models

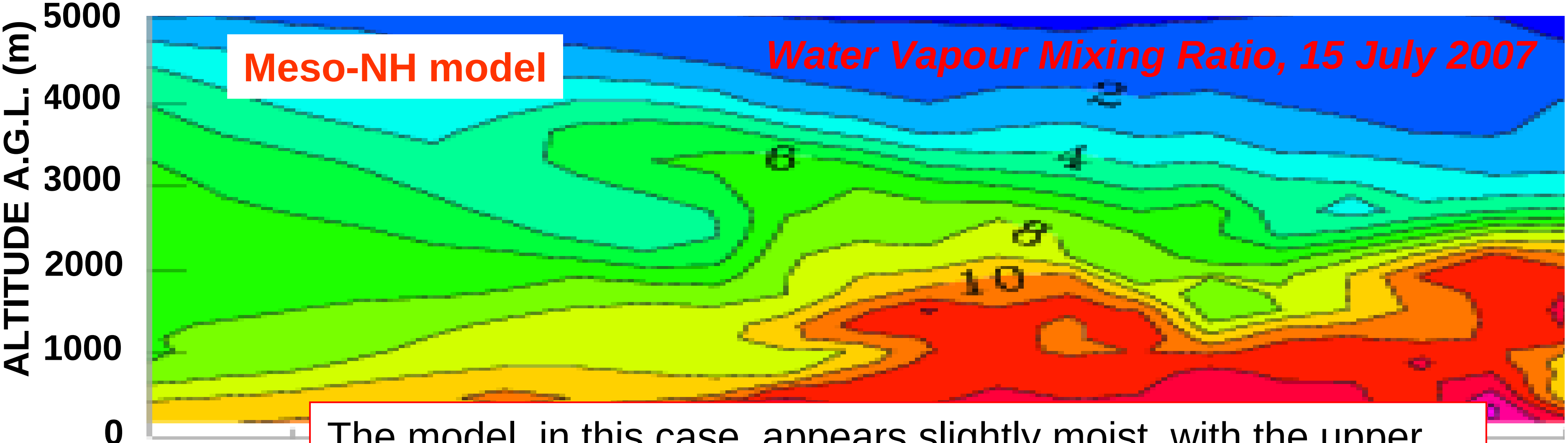

The model, in this case, appears slightly moist, with the upper humid layer extending higher up (4 km instead of 3 km)

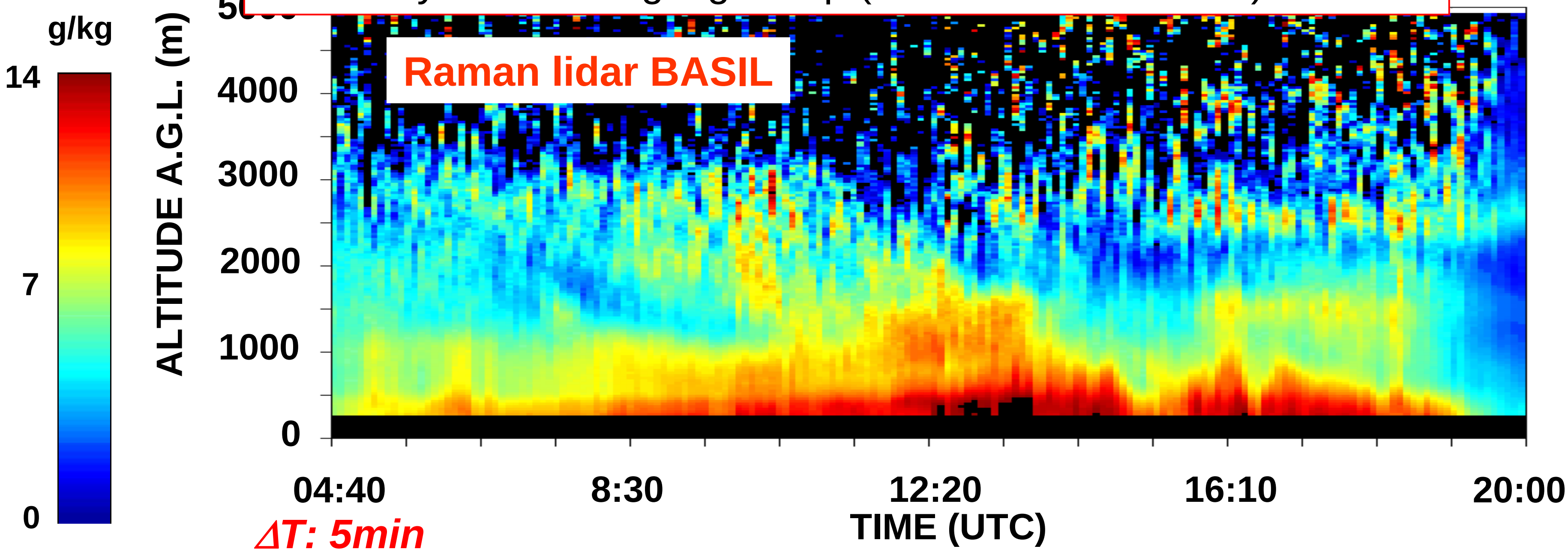

Water vapour inter-comparison effort

Comparison of measurements (quality assurance) from different water vapour remote sensing systems. Assessment of accuracy and precision.

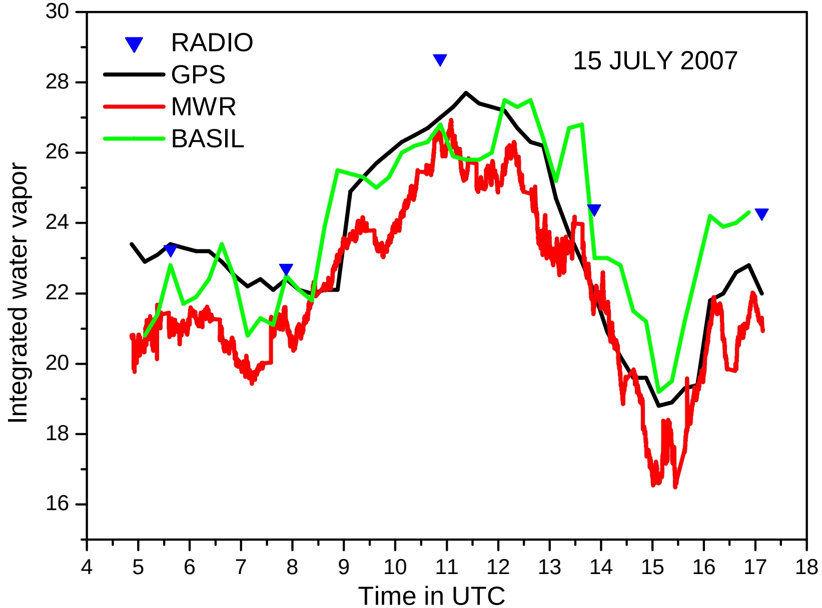

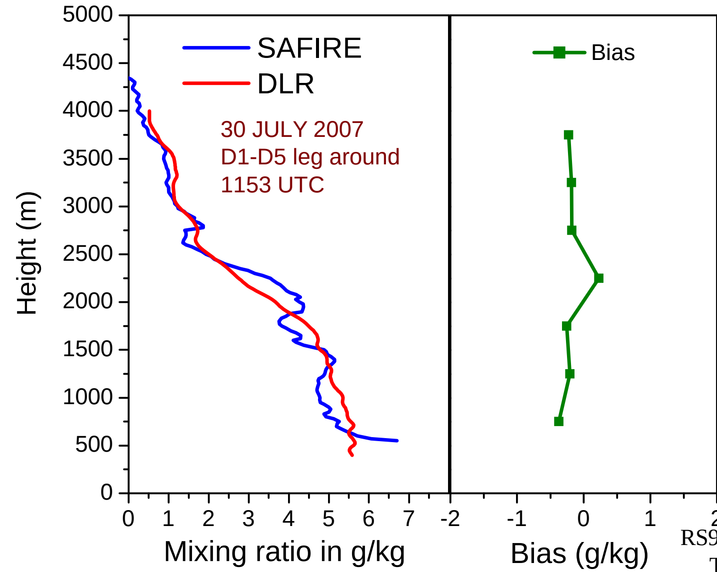

IGN Raman Lidar vs CNRS DIAL

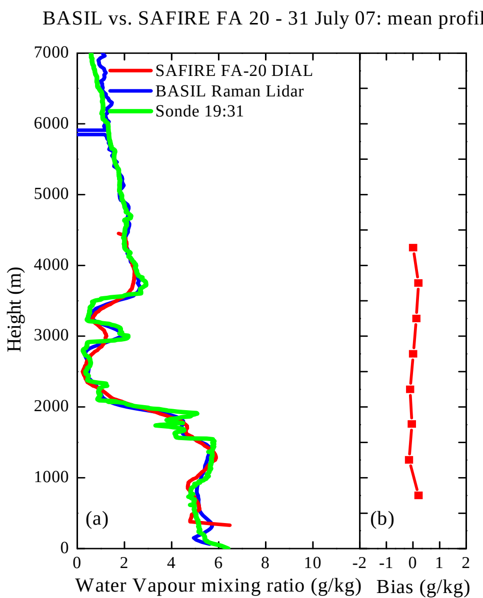

IGN Raman Lidar vs CNRS DIAL

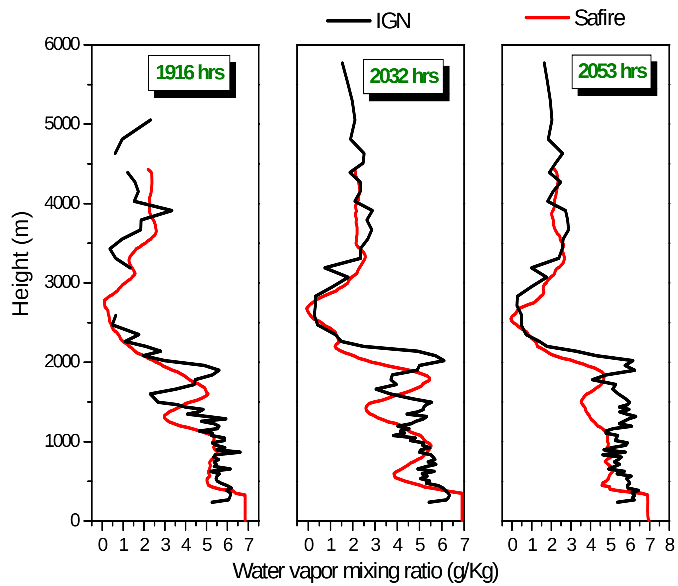

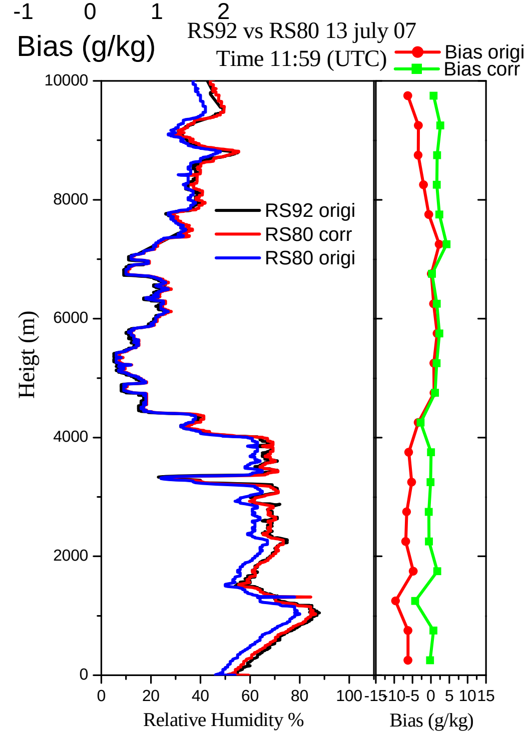

IOP 9c – 20 July 07

Passage of the frontal zone, with a Mesoscale Convective System inbedded

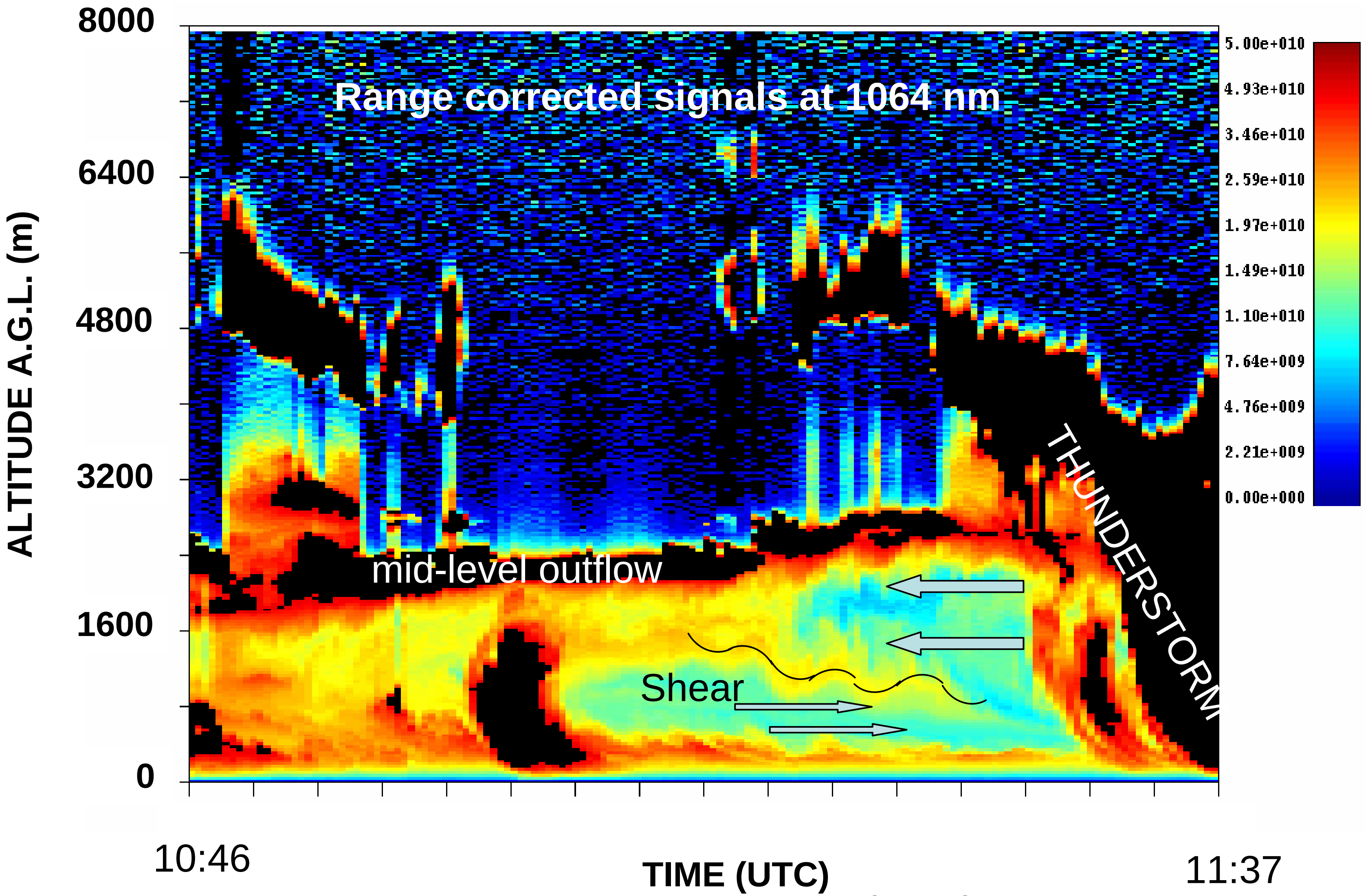

Cloud deck at 2 km represents a mid-level outflow from the thunderstorm/MCS

The waves like structures seen in the data just prior to the arrival of the thunderstorm are due to shear between inflow and outflow regions.

Upper tropospheric humidity and its relation to deep convection and high clouds

BASIL – Rhine Valley Supersite (Lat: 48.64 ° N, Long: 8.06 E, Elev.: 140 m)

25-26 July 2007 – Water vapour mixing ratio

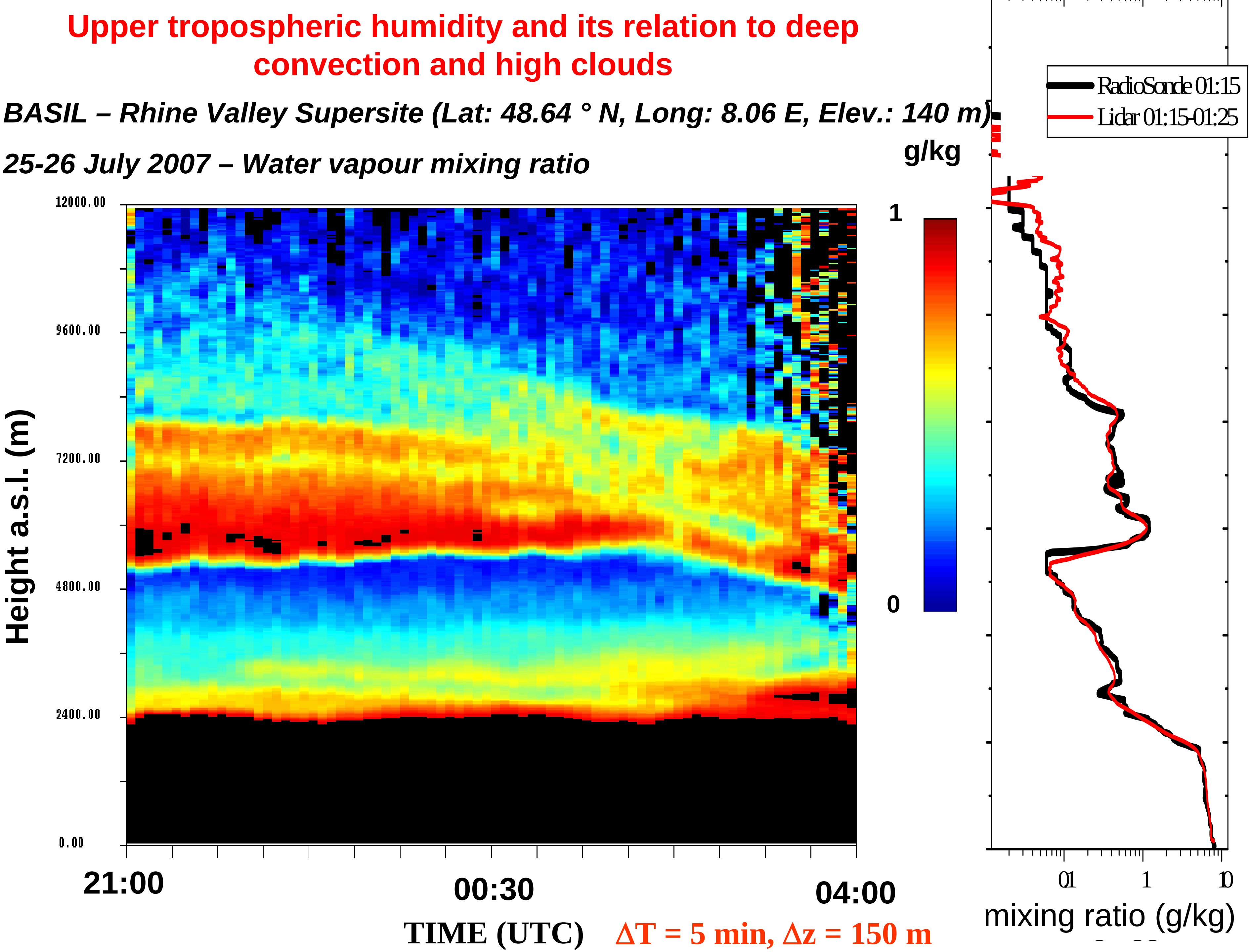

Current reserach topics

- **Raman Lidar observations of a Saharan dust outbreaks: determination of size and microphysical particle parameters.**
- **Lidar and radar measurements of the melting layer: observations of dark and bright band phenomena.**
- **Study of the evolution of MCSs based on Raman Lidar observations of particle backscatter, water vapour and temperature.**
- **Comparison of measurements (quality assurance) from different water vapour remote sensing systems. Assessment of accuracy and precision, and comparability of meteorological data.**
- **Comparison on water vapour and aerosol measurements from Raman lidar with runs from Meso-NH model and other mesoscale models.**
- **Upper tropospheric humidity and its relation to deep convection and high clouds**